Fault Patterns at Outer Trench Walls

D. G. MASSON

Institute of Oceanographic Sciences Deacon Laboratory, Wormley, Surrey GU8 5UB, U.K.

(Received 8 February, 1990; accepted 30 January, 1991)

Key words: Normal faults, trenches, subduction, oceanic crust, GLORIA.

Abstract. Profiles across subduction-related trenches commonly show normal faulting of the outer trench wall. Such faulting is generally parallel or sub-parallel to the trench and is ascribed to tension in the upper part of the oceanic plate as it is bent into the subduction zone. A number of authors have noted that outer trench wall faulting may involve re-activation of the oceanic spreading fabric of the subducting plate, even when the trend of this fabric is noticeably oblique to the extensional stress direction. However, one previous review of outer trench wall fault patterns questioned the occurrence of a consistent link between fault orientation and such controlling factors. This latter study pre-dated the widespread availability of swath bathymetry and long-range sidescan sonar data over trenches. Based only on profile data, it was unable to analyse fault patterns with the accuracy now possible. This paper therefore re-examines the relationship between outer trench wall faulting and the structure of the subduction zone and subducting plate using GLORIA and Seabeam swath mapping data from several locations around the Pacific and Indian Oceans. The principal conclusion is that the trend of outer trench wall faults is almost always controlled by either the subducting slab strike or by the inherited oceanic spreading fabric in the subducting plate. The latter control operates when the spreading fabric is oblique to the subducting slab strike by less than 25–30°; in all other cases the faults are parallel to slab strike (and parallel or sub-parallel to the trench). Where the angle between spreading fabric and slab strike is close to 30°, two fault trends may coexist; evidence from the Aleutian Trench indicates a gradual change from spreading fabric to slab strike control of fault trend as the angle between the two increases from 25 to 30°. The only observed exception to the above 'rule' of fault control comes from the western Aleutian Trench, where outer trench wall faults are oblique to the slab strike, almost perpendicular to the spreading fabric, and parallel to the convergence direction. Re-orientation of the extensional stress direction due to right-lateral shear at this highly oblique plate boundary is the best explanation of this apparently anomalous observation.

Introduction

Bathymetric and seismic reflection profiles across subduction-related trenches commonly shown distinctive patterns of normal faulting on the outer trench wall, i.e. in the subducting oceanic plate (Figures 1, 2). It is generally accepted that such faulting results from tensional stresses in the upper part of the oceanic plate where it bends into the subduction zone (e.g. Ludwig *et al.*, 1966; Jones *et al.*, 1978). Hilde (1983) reviewed the occurrence of outer trench wall faulting around the Pacific and found it to be essentially ubiquitous in areas where the sedimentary cover on the subducting plate is thin (<400 m). Where thicker sediments occur, he suggested that these could mask faults within the underlying basement, although the mechanism by which masking would occur was not specified.

Published descriptions of faults in outer trench walls generally indicate that they are parallel or sub-parallel to the adjacent trench axis (Jones *et al.*, 1978; Hilde, 1983). Obvious factors which might control the trend of such faults include the strike of the subduction zone (which is perpendicular to the principal tensional stress developed as a result of bending of the subducting lithosphere), and any weakness in the subducting plate, for example the oceanic spreading fabric. Reactivation of the oceanic spreading fabric has been cited by several authors as an explanation for obliquity between outer trench wall fault trends and the apparent tensional stress trend at several locations around the Pacific Ocean (e.g. Jones *et al.*, 1978; Aubouin *et al.*, 1982, 1984; Scholl *et al.*, 1982; Cadet *et al.*, 1987). However, in a worldwide review of this topic, Hilde (1983) questioned the occurrence of any *consistent* control of this nature. He found that faults could be parallel or oblique to trenches, could cut across magnetic lineations and spreading fabric trends, and were not necessarily perpendicular to convergence directions. However, Hilde's study pre-dated the wide availability of swath-bathymetric and long range sidescan sonar data over deep-sea trenches. Such

Marine Geophysical Researches **13**: 209–225, 1991.

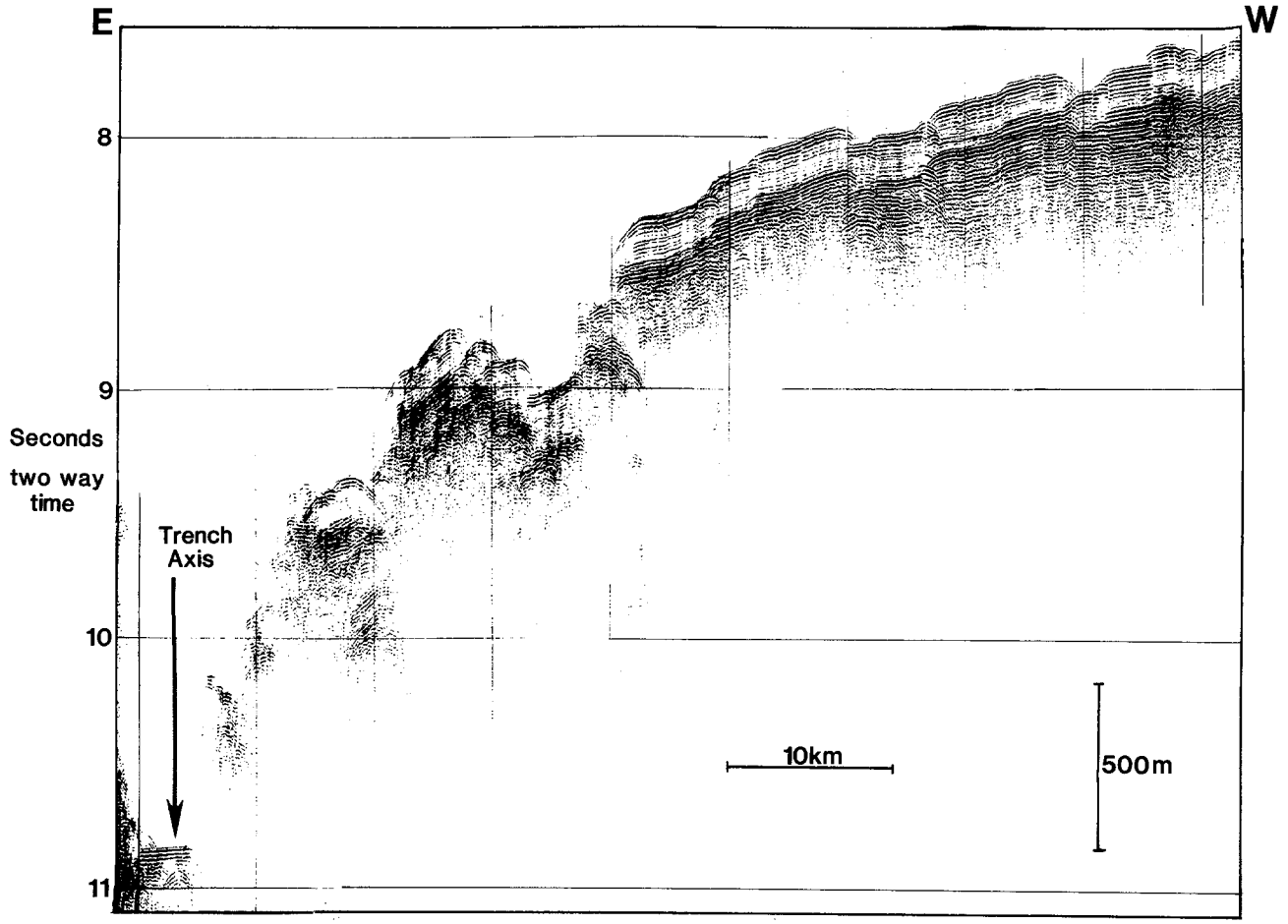

Fig. 1. Seismic reflection profile across the Tonga Trench showing extensional normal faulting. Note the increase in fault throw and the increasing dominance of trenchward-throwing faults toward the trench.

data, now widely available, allows a more accurate and more detailed analysis of fault trends than was possible using only profile data. This paper therefore re-examines the relationship between outer trench wall faulting and the structure and geometry of the subduction zone and subducting plate. It is based on GLORIA long-range sidescan sonar data from the Aleutian, Java, Peru and Tonga Trenches, complemented by published Seabeam bathymetric data from the Middle America, Japan, Kuril, Izu-Bonin and Tonga Trenches (Figure 3).

General Observations

Fault parameters for the areas studied are summarised in Table I and illustrated in Figure 2. Many are remarkably consistent between the various areas. In particular, the length of individual fault segments is typically 5–30 km, rarely extending to 60 km; fault spacing is usually 1–10 km; the fault zone usually extends some 50–75 km seaward of the trench. It might be expected that these fault zone parameters might vary with the slope of the subducting plate; i.e., with the degree of bending to which the subducting plate is subjected. However, the only parameter which appears to vary in this way is fault throw, which increases with increased bending of the plate (Jones *et al.*, 1978). This is well illustrated by Figure 2 which shows average fault throw increasing from <35 m at the Peru Trench, where the plate slope is $<3°$ immediately seaward of the trench, to about 115 m at the Aleutian Trench, where the plate slope reaches 9°.

A further point worthy of discussion is the development of fault patterns as an oceanic plate moves toward a trench. In all the examples studied here,

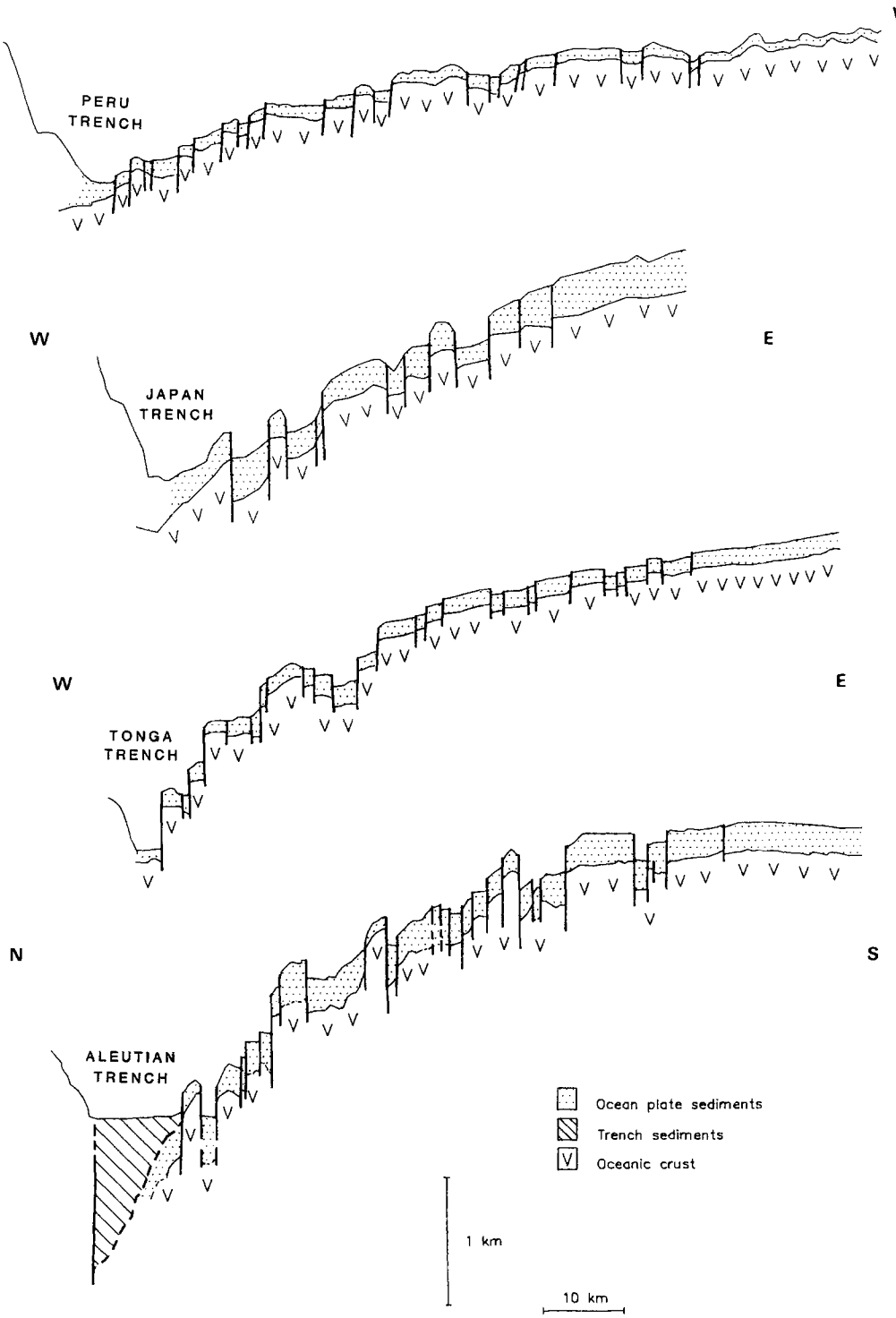

Fig. 2. Interpreted seismic profiles across four Pacific Ocean trenches.

faulting initially creates symmetrical horst and graben structures at distances up to 75 km from the trench axis (Figure 2). This symmetry is maintained while the plate moves to within about 30 km of the trench axis, with cumulative curves of fault throw showing approximately equal throw towards and away from the trench (Figure 4). However, within 30 km of the trench axis, faults throwing toward the

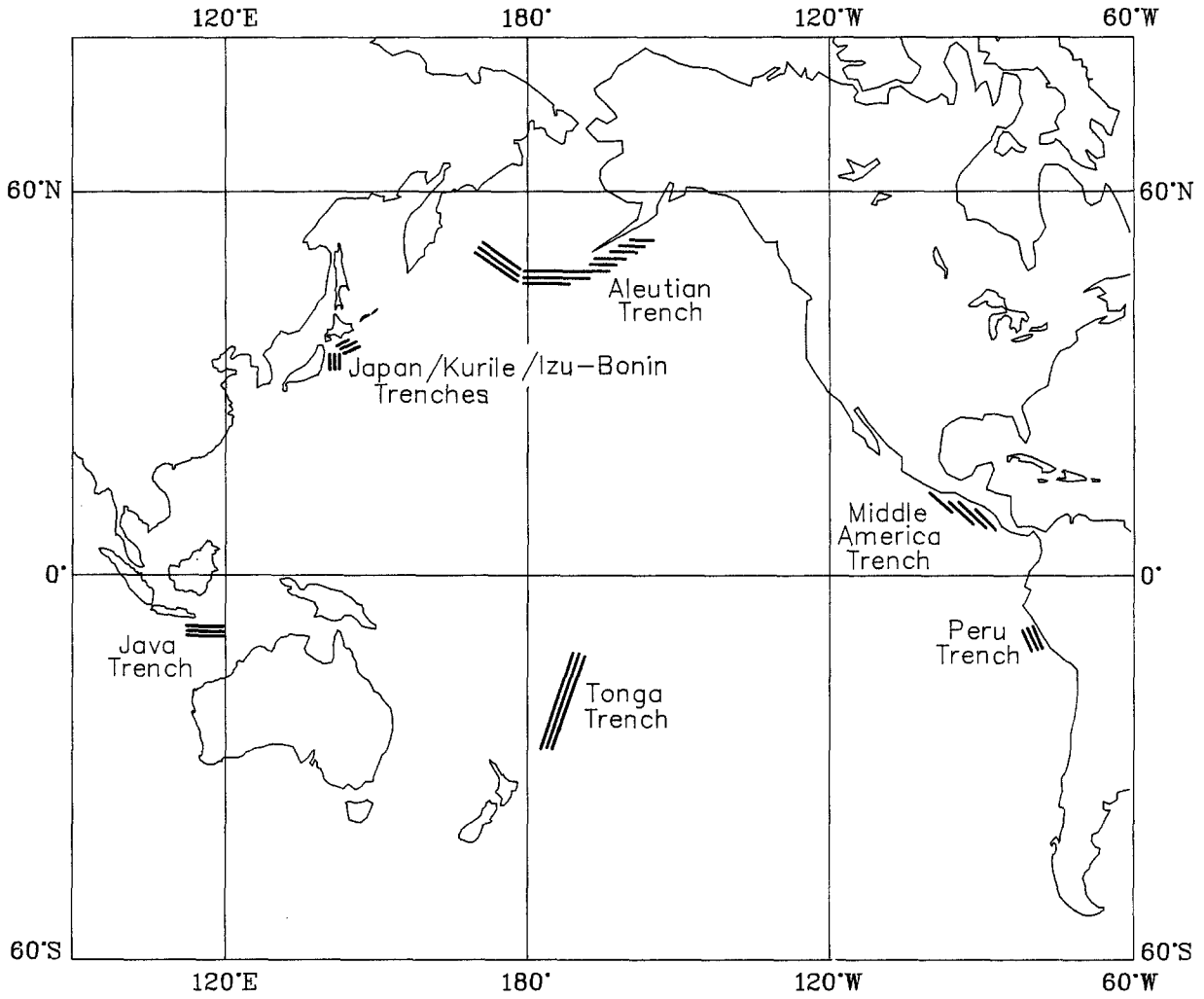

Fig. 3. Location of areas studied. Shading indicates approximate trend of outer trench wall faults in each area.

trench become dominant (Figures 2, 4). This has been noted previously by Cadet *et al.* (1987) and Moore and Shipley (1988) for the Japan and Middle America Trenches respectively, but is confirmed by all the examples studied here. This suggests that faulting is initially created by bending stress, which should produce symmetrical fault patterns as concluded by Jones *et al.* (1978), but that other stresses become more influential near the trench axis. Although full treatment of this observation is beyond the scope of this paper, one potential source of stress which could produce the observed asymmetry of faulting near the trench axis is loading by the overriding plate, as originally suggested by Ludwig *et al.* (1966).

Orientation of Outer Trench Wall Faults: New Observations and Data Analysis

The Aleutian Trench

GLORIA long-range sidescan sonar data covering the entire United States Exclusive Economic Zone south of the Aleutian Islands is by far the biggest data set pertinent to the present study. This survey gives complete coverage of the Aleutian margin, and of the oceanic plate out of some 200 km seaward of the trench axis, between 150° W and 170° E, a distance of some 2700 km. Extensional faulting of the outer trench wall is seen along most of the trench, between 170° E and 157° W, but disappears east of

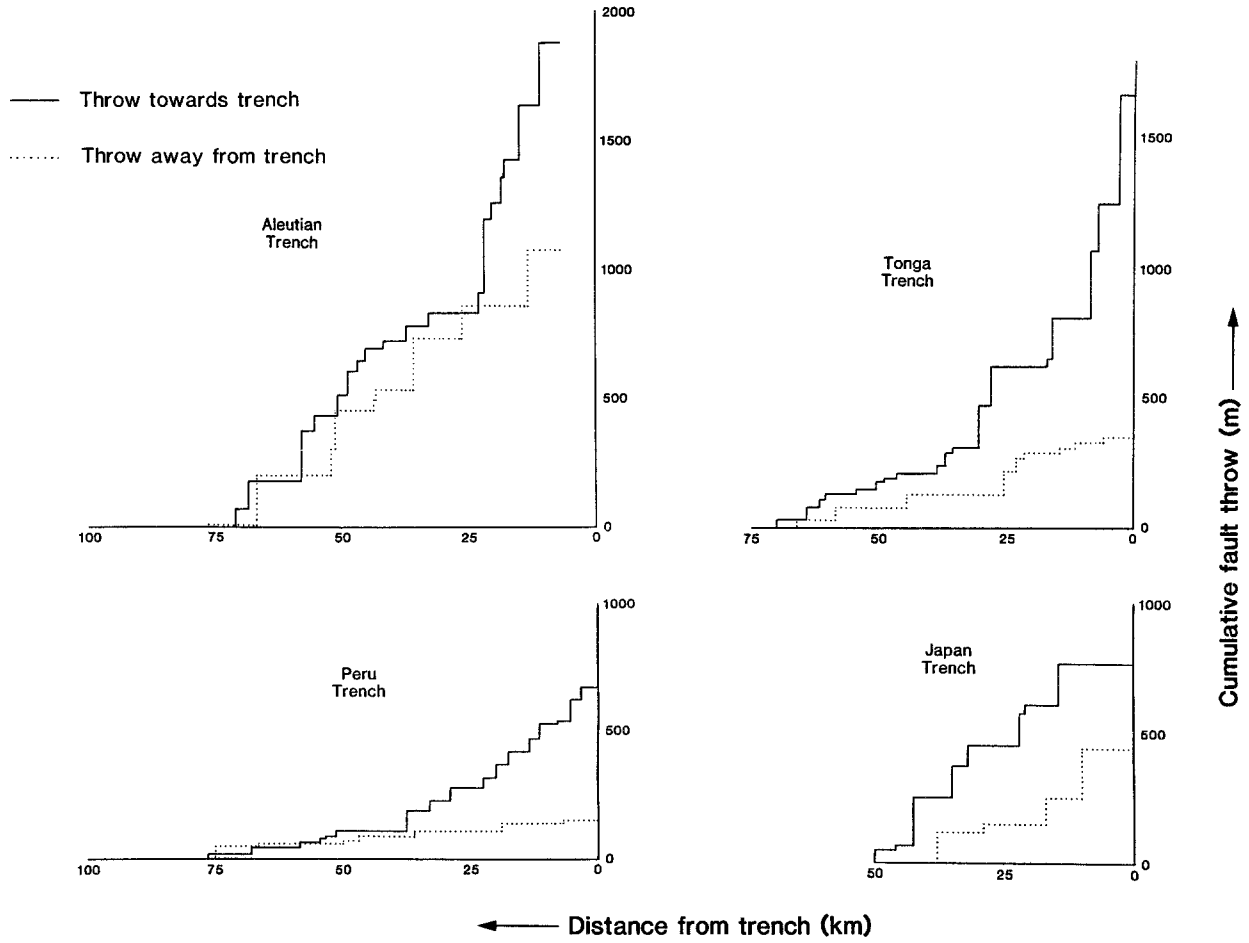

Fig. 4. Cumulative fault throw against distance from the trench for the four profiles shown in Figure 2. This clearly shows that faulting initially forms symmetrical graben at distances of up to 75 km from the trench, but that trenchward throwing faults become dominant within 30 km of the trench.

157° W as the sediment cover on the subducting Pacific Plate thickens toward the Alaskan mainland margin. Typically, the zone of extensional faulting extends 40 to 75 km seaward of the trench (Figures 5, 6, Table I). Fault throws reach a maximum of about 400 m close to the trench, fault spacing is typically 1 to 10 km, and individual fault segments can reach 50 km in length (Figures 5, 6, Table I).

The following analysis of fault trends is based on some 2500 trend measurements on individual fault segments. Fault trends were measured using a digitising tablet with each fault approximated to a straight line or series of straight line segments. No attempt was made to weight the importance of faults according to their length or throw; each straight line segment simply constituted one data point.

The primary data set is presented as a series of rose diagrams, each covering one degree of longitude (Figure 7). These clearly show the main characteristics of the extensional fault zone. The most obvious feature is the abrupt change in fault trend, by some 35°, at 179° E. West of this point, faults cluster round a trend of 120–130°; to the east, the principal trend is around 90° (Figures 7, 8). This change of trend is also accompanied by a change in character of the fault zone. To the west, fault trends typically cover an arc of 30–35°, but to the east the range of trend is much narrower, with most faults falling in a 15–20° arc. This change is very clearly shown in the histograms of Figure 9.

More subtle changes in fault pattern occur between 179° E and the eastern end of the extensional fault zone at 157° W. For some 12° of longitude east

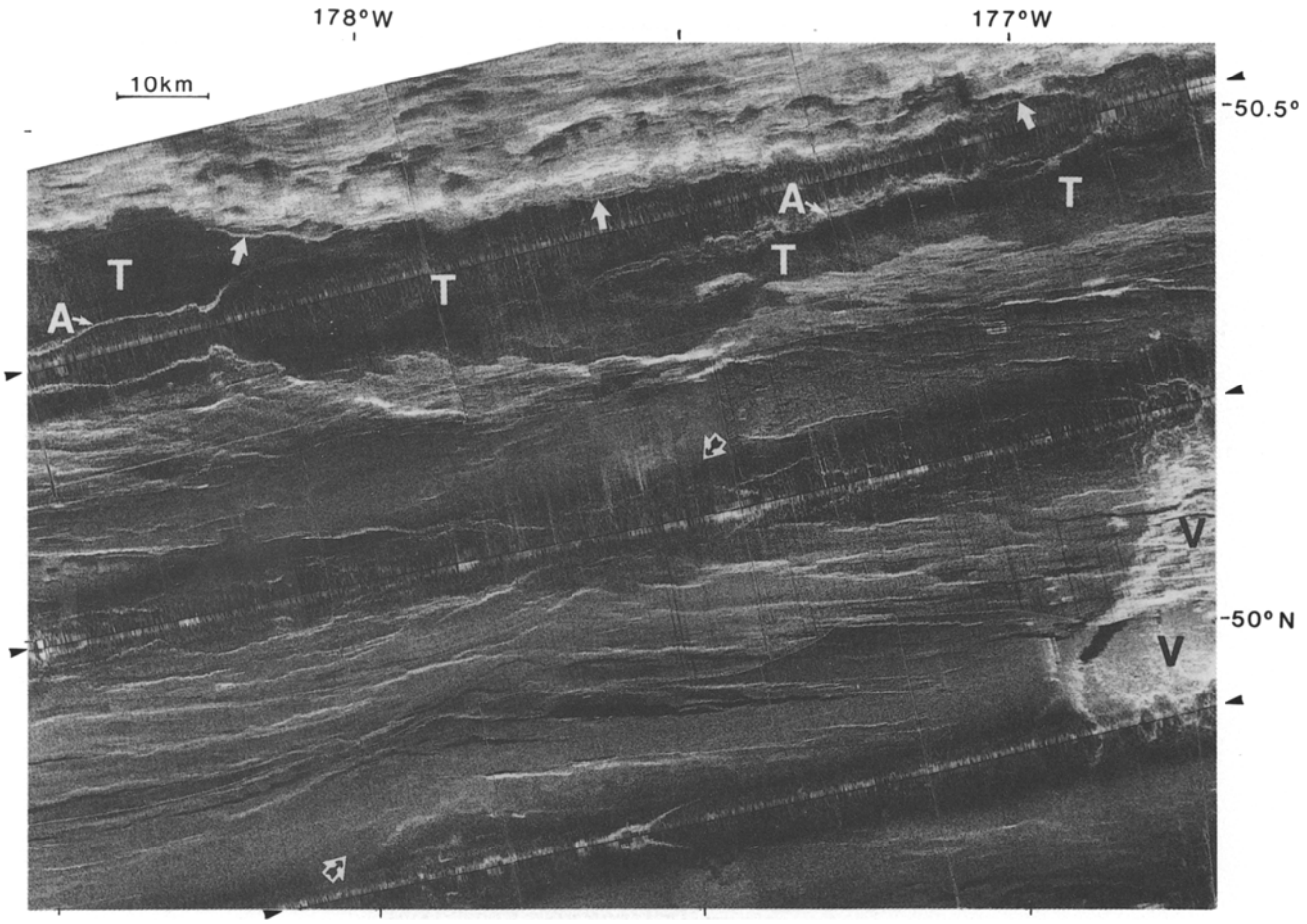

Fig. 5. Example of GLORIA long-range sidescan sonar data from the Aleutian Trench and outer trench wall fault zone. Dark areas = low backscatter. T = flat sedimented trench floor; A = artefact caused by interference between two sides of sonar. Large 'black in white' arrows mark reactivated spreading fabric associated with pseudofault trace; plain white arrows show deformation front; arrowheads around border show ships tracks. For full interpretation see Figure 6.

of 179° E, fault trends continue to cluster around 90°, and the range of fault trends remains small, covering 15–20° of arc (Figures 7, 9). Small excursions from this consistent situation occur between 177° and 178° W and 172° and 173° W, where significant numbers of faults have trends of less than 90° (Figure 7). This is most easily seen in the average fault trend plot where localised points lower than the typical average value of 85–90° are seen (Figure 8).

Eastward from 169° W, the proportion of faults with trends of less than 90° gradually increases (Figure 7), leading to a gradual decrease in the average fault trend (Figure 8). However the simple average used in Figure 8 hides the true reasons for this decrease. Firstly, examination of the raw data clearly shows the development of a subsidiary ENE fault trend which becomes more important eastward (Figure 7). Secondly, when the data are plotted in histogram form, the distribution of fault orientations within the major (E–W) trend is seen to be strongly skewed towards values less than 90° (Figure 9). This compares with an almost perfectly symmetrical distribution between 179° E and 169° W (Figure 9).

Figures 8 and 9 show fault trend variation with longitude plotted against possible controlling factors. In practice, there would appear to be only two such factors: subduction geometry and inherited structural weaknesses in the subducting plate, but these can be measured in a variety of ways, depending on the data available. For subduction geometry, the strike of the subducting slab (i.e. the perpendicular to the direction of maximum bending stress) is best determined from contoured earthquake hypocentre plots or gravity anomaly maps (e.g. see AAPG, 1984 and Stone, 1988, for the Aleutian Arc). The trend of the trench can also be used as a guide to the

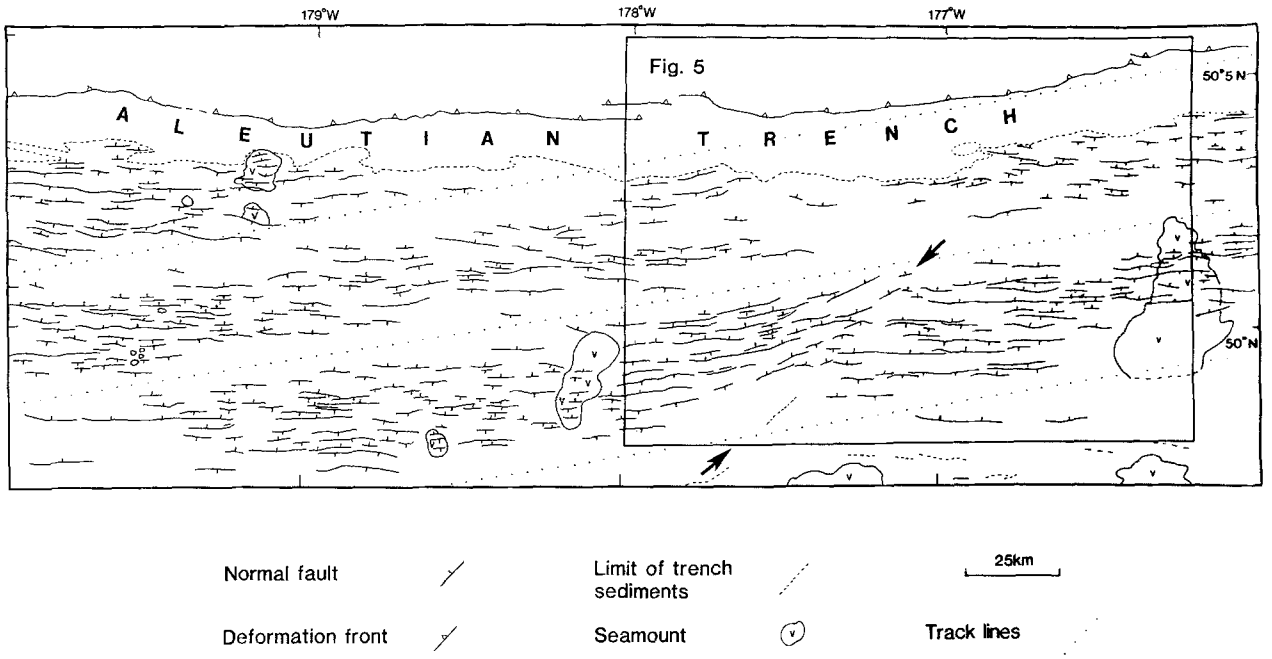

Fig. 6. Interpretation of GLORIA data from part of the Aleutian Trench. Fault trends digitised from line drawings of this type formed the raw data set for the construction of Figures 7–9. Large arrows show pseudofault trace. Box shows area of Figure 5.

TABLE I

Fault zone characteristics for the areas studied

Trench	Fault throw (m)	Fault length (km)	Fault spacing (km)	Width of fault zone (km)	Oceanic plate slope (°)
Aleutian	up to 400	5–30 (50)	1–10	40–75	7–9
Java	100–500	5–20 (60)	2–10	50	2.5–4
Peru	up to 200 (500)	5–25 (50)	1–15	50–75	2–3
Middle America	100–200	10–20	0.5–10	?	2.5–4
Izu-Bonin	up to 500 (1000)	5–30 (50)	1–10	50+	3–6
Japan/Kuril	up to 500	5–60	2–10	50	3–5
Tonga/Kermadec	100–500 (1000)	up to 50	1–10	60	5–8

subduction geometry, if measured over a segment of trench long enough to average out local irregularities in trench trend such as those seen in Figure 8. For inherited weaknesses, structural trends in the subducting oceanic plate can be measured directly from sidescan sonar or swath bathymetric data, if available. Alternatively, the major structural trend in oceanic crust, the inherited mid-ocean ridge spreading fabric, can be estimated from magnetic anomaly trends.

For the Aleutian Trench, controls on outer trench wall faulting are most easily discussed in terms of the three trench segments shown in Figure 9. In the central segment, between 179° E and 169° W, the average fault trend closely follows the inherited oceanic spreading fabric as defined using GLORIA data from the area seaward of the fault zone (Figure 8). In the western part of this central segment, the fault trend also coincides with the strike of the subducting slab, but these two trends become markedly divergent eastward (Figure 8). This divergence strongly suggests that it is the inherited spreading fabric rather than subducting slab strike which is controlling the fault orientation. Further evidence

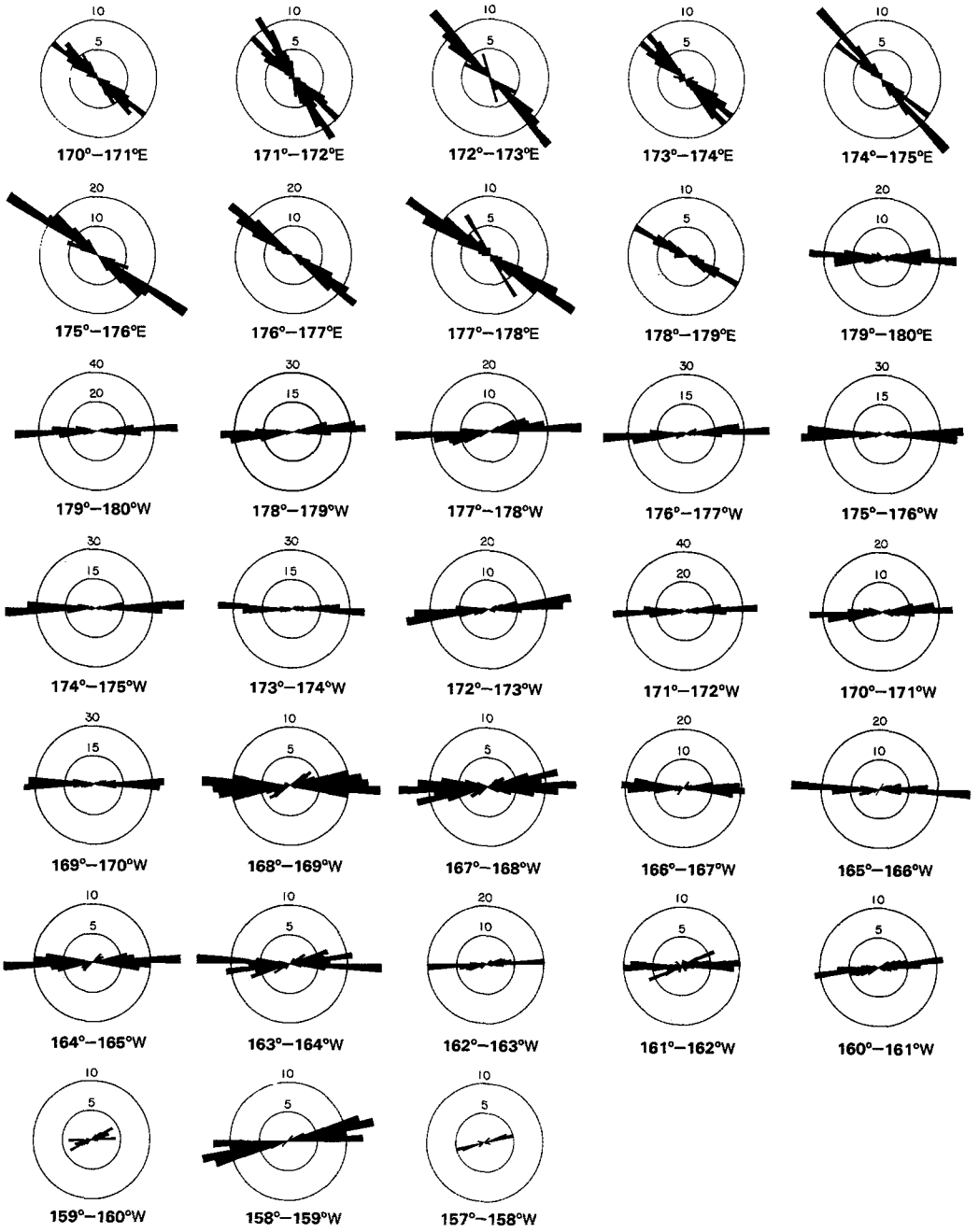

Fig. 7. Fault trends in the Aleutian Trench outer trench wall fault zone displayed in 1° longitude intervals. Numbers on circles indicate number of fault trends measured.

for control of fault trend by the spreading fabric comes from study of the two 1° longitude areas of the central trench segment which give anomalously low average fault trend values (arrows on Figure 8). These low values result from re-activation of ENE deflections of the spreading fabric (Figures 5, 6) which are associated with pseudofault traces (Hey, 1977). They clearly demonstrate a detailed control of fault trend that cannot be attributed to the subducting slab geometry.

East of 169° W, a more complex relationship between fault orientation and controlling parameters can be seen. As described earlier, two fault trends are developed in this area (Figure 7). The major E–W trend continues to be controlled by the inherited spreading fabric, as it is in the area to the west

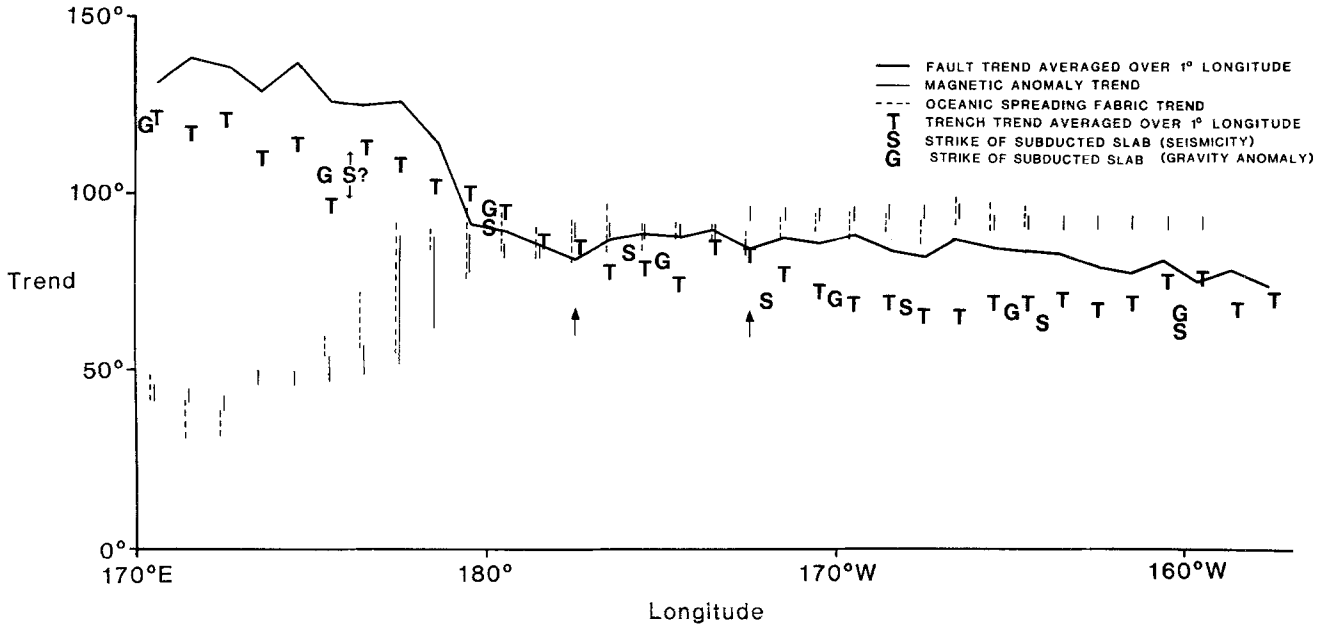

Fig. 8. Fault trends at the Aleutian Trench, averaged over 1° longitude intervals, and plotted against magnetic anomaly and oceanic spreading fabric trends, trench trend, and strike of the subducting slab. Arrows between 170° and 180° W show location of pseudofaults.

(Figure 9). The minor ENE trend appears to parallel the strike of the subducting slab. Note, however, that this minor trend becomes more important eastward, so that east of 160° W it becomes the dominant trend (Figure 7). The distribution of faults within the major E–W trend is also strongly skewed towards values of less than 90°, in contrast to the symmetrical distribution seen further west. It is suggested (although not proven) that this reflects preferential re-activation of the more ENE faults within the inherited oceanic fault suite (rather than the creation of a new set of faults of intermediate trend). From this data set, it is concluded that for an outer trench wall dominated by re-activated faults, divergence from perpendicularity between the inherited fault trend and the direction of maximum bending stress will both skew the distribution of fault orientations within that inherited trend and create a new set of faults perpendicular to the direction of maximum stress (see discussion).

The trench segment west of the 179° E is unique in that of all the trenches examined in the present study, it is the only area where the fault trend does not appear to be related to either the subducting slab strike or the inherited spreading fabric. Here, magnetic anomalies are virtually perpendicular to the fault trend of 120–130° (Figures 7–9; Lonsdale, 1988). The subducting slab strike cannot be defined by seismicity, because of a lack of deep earthquakes, but is clearly defined by its associated gravity anomaly, which parallels the trench (AAPG, 1982, 1984; Stone, 1988). The faults are oblique to this gravity anomaly and trench trend by 20–30° (Figure 8). The best explanation for the observed fault trend along this trench segment is that the extreme obliquity of plate convergence at the western Aleutian Trench (e.g. Stone, 1988) modifies the orientation of the bending stress on the subducting plate. The right lateral sense of motion across the trench is clearly compatible with the observed re-orientation of the extensional faults. However, confirmation of this explanation requires its testing at other oblique convergence plate boundaries.

The Peru Trench

Data from the Peru Trench consist of GLORIA and seismic reflection profiles covering the trench and the oceanic plate immediately seaward of it between 10.5 and 13.5° S. This data set has previously been analysed by Warsi *et al.* (1983). These authors concluded that 'bending-induced faults strike sub-parallel to the trench axis and overprint and cut across spreading fabric structures' on the outer trench wall. Although for at least part of the area the strike of the spreading fabric is identical to that of the new bending-induced faults, Warsi *et al.* believed that the

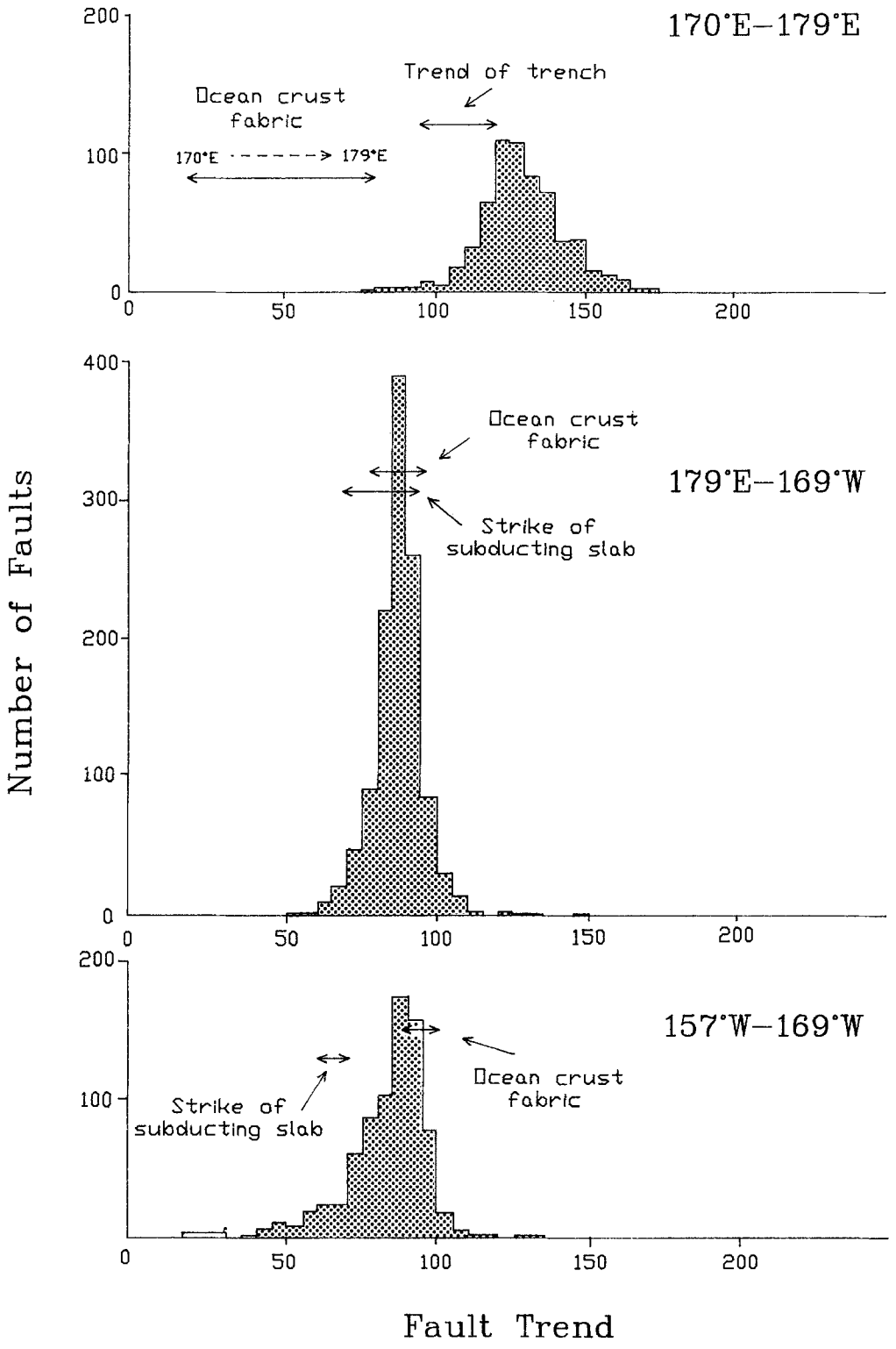

Fig. 9. Fault trends at the Aleutian Trench displayed as histograms for each of three trench segments with differing fault pattern characteristics.

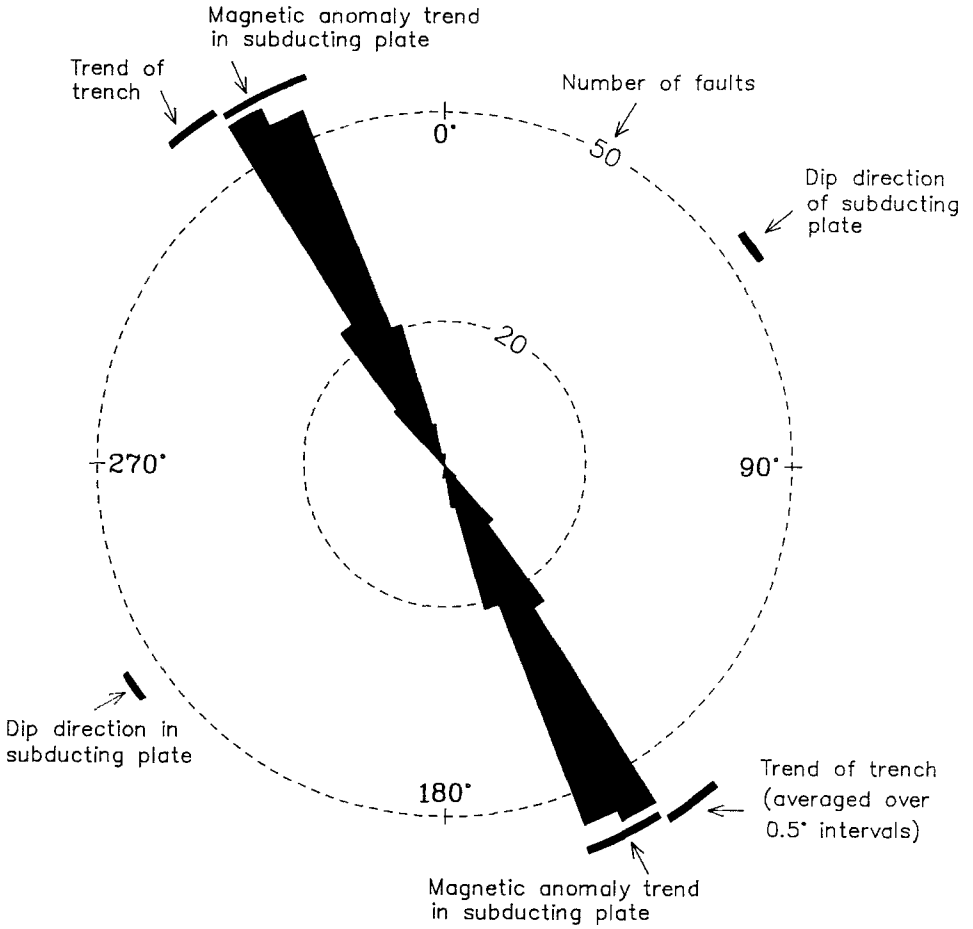

Fig. 10. Fault trends at the Peru Trench between 10.5° and 13.5° S compared with magnetic anomaly and trench trends and the dip of the subducting slab. This example clearly shows control of the fault trend by the oceanic spreading fabric (= the magnetic anomaly trend) even though this differs by only 10° from the subducting slab strike.

two fault sets could be differentiated on GLORIA data. Nowhere do they suggest that old spreading fabric faults might be re-activated.

A re-interpretation of the Peru Trench data is given in Figure 10. On the basis of trend alone it is clearly possible to distinguish a new set of bending induced faults. Indeed, the exact correlation in trend between measured faults and magnetic anomalies (Table II; Pilger, 1983), would suggest complete control of the bending induced faulting by the inherited spreading fabric weakness. This conclusion is reinforced by the fact that there is no obvious fault trend parallel to the strike of the subducting slab (Barazangi and Isacks, 1976), even though this differs by only about 10° from that of the magnetic anomalies. Furthermore, the narrow range of fault trend ($<20°$ of arc in Figure 10) at the Peru Trench is very similar to that seen at the central segment of the Aleutian Trench where spreading fabric re-activation occurs, but much narrower than at the rest of the Aleutian Trench where a new set of faults is formed.

The Java Trench

A single GLORIA swath along a 1300 km length of the eastern Java Trench images limited areas of the subducting oceanic plate which are cut by outer trench wall faulting (Masson *et al.* 1990). A summary of the data obtained from this swath is given in Figure 11. Faults are parallel to both the trench trend and the strike of the subducting slab (McCaffrey *et al.*, 1985), but oblique to the magnetic anomaly trend (Heirtzler *et al.*, 1978) by some 30° (Table II; Fig. 11). It is clear, therefore, that the fault trend is controlled only by the bending stress acting on the subducting oceanic plate. A characteristic of

TABLE II

Summary of outer trench wall fault trends and possible controlling parameters. Solid underline shows control of major trends, dotted underline control of minor trends

Trench	Fault trend	Trench trend	Magnetic anomaly trend	Slab strike	Slab age	Convergence direction
Aleutian 170–179° E	110–150	095–120	040–085	?	50	130
Aleutian 179 E–170° W	070–100	075–100	080–095	070–090	60	135
Aleutian 157–170° W	075–100 (major) 055–075 (minor)	065–078	092–098	060–070	55	140
Java 108–120° E	075–110	075–105	060	090	135	020
Peru 10–14° S	145–165	140–145	150–160	140–145	45	080
Middle America 15.5–16.5° N	120–135	110	130	100–110	12	045
Middle America 12.5–13° N	130–150 (major) 105–120 (minor)	112	?140	120	30	045
Middle America 9.5° N	120–140	135	?	130	?	045
Izu–Bonin 33–35° N	160–180 (major) 020–040 (minor)	170–190	035	170	140	110
Japan 36–40.5° N	350–030	005–020	065	010	120	110
Kuril 41° N	055–065	060	065	060	120	115
Tonga/Kermadec 16–27.5° S	000–020	000–030	080	170	140	100

the Java Trench faults is the relatively wide range of trends that occur (35° of arc in Figure 11). This may result in part from summing several small data sets from a lengthy trench segment, although no systematic variation in fault trend along the trench is visible in the raw data. Disruption of fault patterns around subducting seamounts may also contribute (Masson *et al.*, 1990). However, wide ranges of fault trend (35–40°) appear to be a general characteristic of outer trench walls where a new set of faults is formed; in contrast, outer trench walls with re-activitated faults show narrower ranges ($\sim$20°, Table II).

The Tonga/Kermadec Trench

Data from the Tonga/Kermadec Trench consists of a reconnaissance swath bathymetry survey along the trench axis between 12 and 26° S (Lonsdale, 1986) and two sub-parallel GLORIA swaths along the trench axis and the oceanic area immediately seaward of the axis between 24 and 27.5° S (Parson, 1989; Jacobs, pers. comm. 1989). A summary of outer trench wall fault trends picked from the GLORIA data is given in Figure 12 and other relevant parameters are given in Tables I and II. These data show that the faults are parallel or sub-parallel to

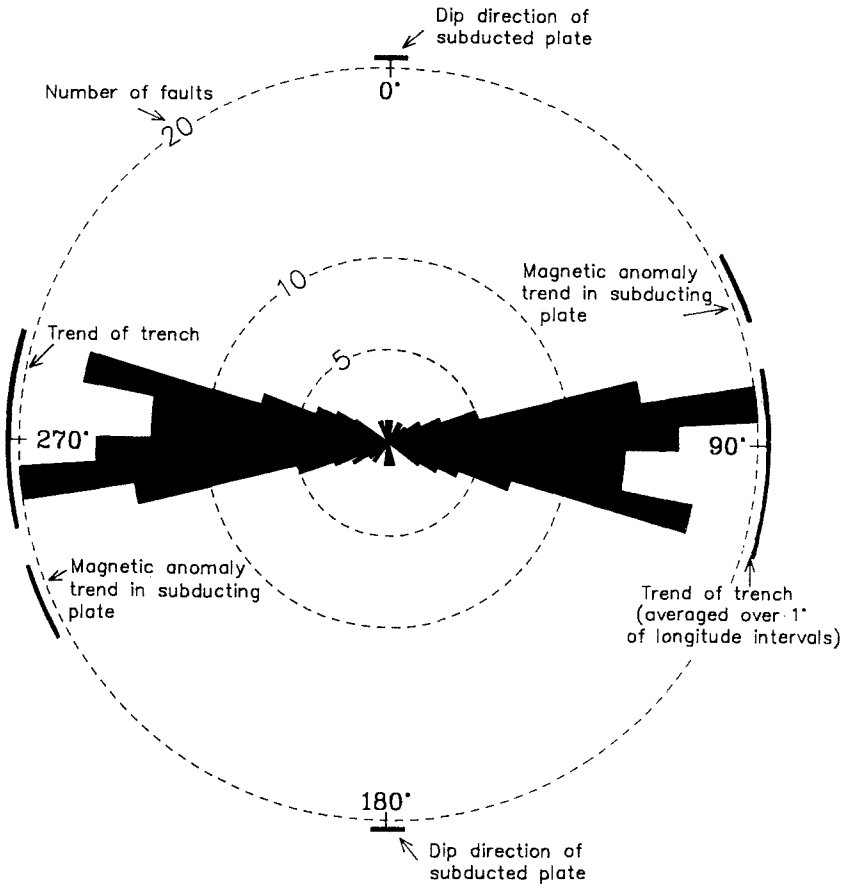

Fig. 11. Fault trends at the Java Trench between 108° and 120° E compared with magnetic anomaly and trench trends and the dip of the subducting slab. Here, fault trend is controlled by the subducting slab strike; the magnetic anomaly trend, which differs from this direction by 30°, has no influence.

both the trench trend and the strike of the subducting slab, but distinctly oblique to the oceanic spreading fabric (Figure 12; Lonsdale *et al.*, 1986). As for the Java Trench, a wide range of fault trends is observed (Figure 12).

The Middle America Trench

Three areas of Seabeam swath bathymetry give outer trench wall fault trends at the Middle America Trench at ~9.5°, 12.5–13° and 15.5–16° N (Shipley and Moore, 1985; Moore and Shipley, 1988). Magnetic anomaly trends are given by Shipley *et al.* (1980) and Klitgord and Mammerickx (1982), and subducting slab geometry by Nixon (1982) and Vasicek *et al.* (1988). At the northern site, fault trends are parallel to magnetic anomalies and oblique to the subducting slab strike by 20–25° (Table II). At the central site, two fault trends are observed—a major trend oblique to the slab strike by about 20°, and a minor trend parallel to the slab strike (Table II). Magnetic anomalies have not been identified in this area, but if it is assumed that they are approximately perpendicular to known fracture zone trends (Klitgord and Mammerickx, 1982), then they would be parallel to, and the controling influence on, the major fault trend. At the southern site, the faults are sub-parallel to the slab strike; magnetic anomaly trends are unknown in this area (Table II).

The Middle America Trench therefore confirms the major observations made at the Aleutian Trench, i.e., that inherited weaknesses in the subducting oceanic plate control the orientation of outer trench wall faulting if they are oblique to the strike of the subducting slab by less than 20–30°; beyond that obliquity, a new set of faults parallel to the slab strike are formed.

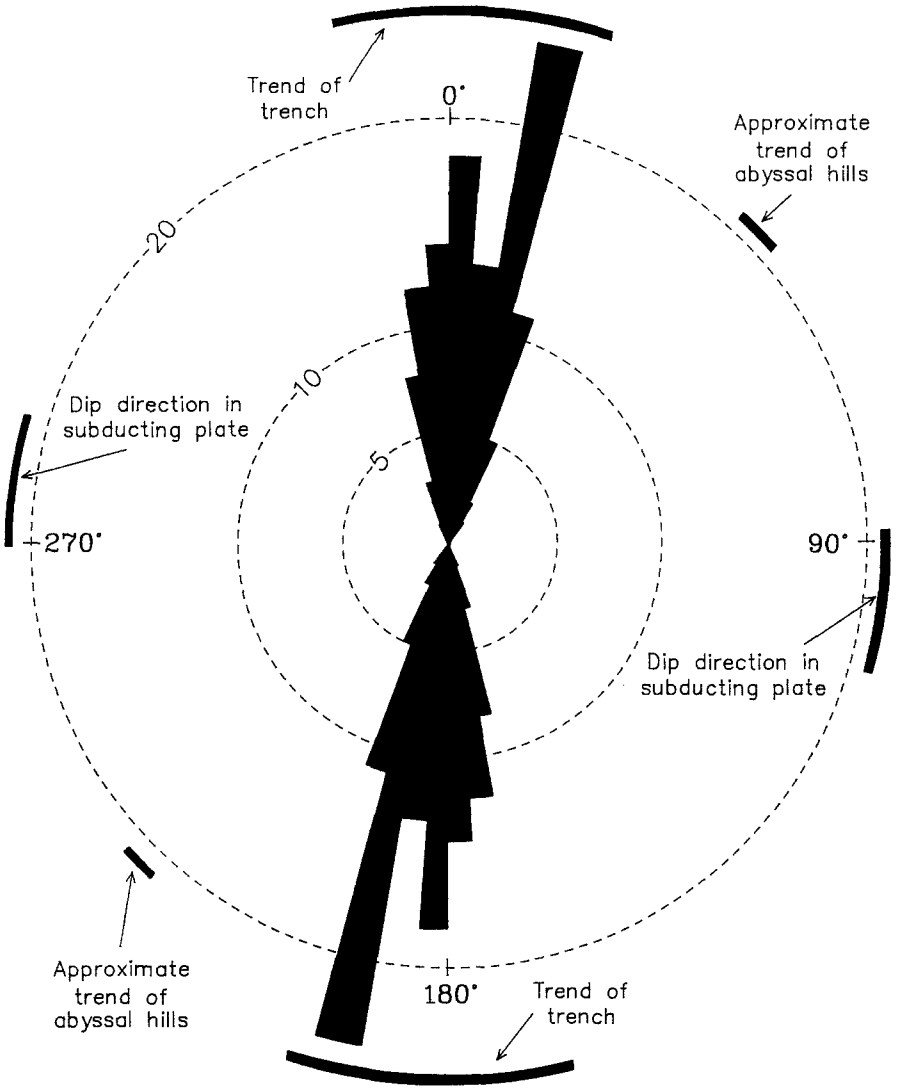

Fig. 12. Faults trends at the Tonga Trench between 24° and 27.5° S compared with magnetic anomaly and trench trends and the dip of the subducting slab. In this example, fault trend is controlled by subducting slab strike.

The Japan/Kuril/Izu-Bonin Trench

Outer trench wall faulting is seen in three areas of Seabeam swath bathymetry in the NW Pacific, one between 33 and 35° N at the Izu-Bonin Trench, a second at 36° N at the Japan Trench, and a third at the junction of the Japan and Kuril Trenches between 39.5 and 41.5° N (Kaiko 1 Research Group, 1986; Renard *et al.*, 1987; Kobayashi *et al.*, 1987; Cadet *et al.*, 1987). Between 33 and 35° N, two fault trends are seen (Table II, Renard *et al.*, 1987). The major trend, 160–180°, is parallel to the strike of the subducting slab (Le Pichon and Huchon, 1987) and oblique to the magnetic anomaly trend (Renard *et al.*, 1987) by about 40°; the minor trend, 020–040°, is parallel to the magnetic anomaly trend. Renard *et al.* (1987) note that, for the most part, the new, approximately N–S, fault trend cuts across the older inherited NE trend. Some N–S graben are offset by NE trending faults, but this may indicate re-activation of the inherited trend as vertical or strike-slip faults rather than as extensional faults. The re-activation is therefore an indirect rather than a direct consequence of the bending-induced extension.

At 36° N, faults trend 030°, parallel to both the trench trend (Kobayashi *et al.*, 1987) and to the strike of the subducting slab (Le Pichon and Huchon, 1987), and oblique to the magnetic anomaly

trend by 35°. The change in fault trend of about 50° (from 160/340° to 030/210°) between 33.5° and 36° N appears to be gradual and has been linked to the 'progressive change in direction of the flexure of the (subducting) Pacific Plate' (Renard *et al.*, 1987). This is further evidence for control of outer trench wall faults by subducting slab strike.

The junction of the Japan and Kuril Trenches at 41° N is marked by a 50° change of both the trench trend and the strike of the subducting slab (Le Pichon and Huchon, 1987). Well to the south of the junction, around 39.5° N, outer trench wall faults trend 350–020° (Cadet *et al.*, 1987), parallel to the strike of the subducting slab (Le Pichon and Huchon, 1987). However, moving north, the fault trend is gradually rotated in a clockwise direction, so that at 40.75° N most faults trend about 045°. This reflects the configuration of the subducting slab as it also changes trend at the Japan/Kuril Trench junction (Le Pichon and Huchon, 1987). Further north again, the fault pattern is interrupted by a large seamount in the trench axis, immediately north of which the faults adjacent to the southern Kuril Trench trend 055–065°, parallel to both the magnetic anomalies and the strike of the subducting slab. Unfortunately, the seamount in the trench axis obscures the exact nature of the fault trend change at the Japan/Kuril Trench junction. It is not clear whether the gradual trend change seen further south continues smoothly northwards or whether an abrupt change occurs as the inherited ocean plate fabric becomes sub-parallel to the bending stress direction and assumes control of the fault trend.

Discussion and Conclusions

A summary of outer trench wall fault trends and possible controlling parameters for the various areas examined during this study is given in Table II. It is immediately clear that these fault trends are virtually always controlled by either the strike of the subducting slab or by the inherited oceanic spreading fabric. This is contrary to the findings of Hilde (1983) who suggested that no such relationship existed. However, the type and quality of the data used in this study allow a much more accurate analysis of fault trends than that which was possible with the data available to Hilde. Accordingly, the conclusions reached here must supersede his earlier conclusions. The data presented in Table II also show that other subduction zone parameters, such as convergence direction and age of the subducting plate, have no obvious influence on outer trench wall fault zones. Fault trends range from parallel to perpendicular to convergence directions. Reactivation of the oceanic speading fabric is seen in crust ranging from 12 to 120 million years in age. However, possible effects due to the subduction of very young crust have not been examined.

The only observed exception to the apparent 'rule' of fault control occurs at the western Aleutian Trench, where the faults are oblique to both the inferred slab strike and the magnetic anomaly trend. This part of the Aleutian trench is unique in this study in that it is the only area in which the convergence direction is at a low angle to the trench. As discussed in the previous section, the best explanation for this observed fault trend appears to be re-orientation of the extensional stress due to right lateral shear.

The relationship between plate bending stress and re-activation of inherited weakness in the subducting plate apparently depends on the angle between the stress direction and the trend of the inherited weakness. In every case where re-activated oceanic spreading fabric controls the outer trench wall fault trend, the angle between that fabric and the subducting slab strike is less than 30°. Re-activated faults at a higher angle (45°) to the slab strike are seen at the Izu-Bonin Trench, but they have been interpreted by Renard *et al.* (1987) as vertical or strike-slip offsets of a new slab-parallel fault set, rather than re-activated extensional faults. Evidence from the Aleutian and Middle America Trenches suggests that slab-parallel and inherited fault trends may coexist where the obliquity between the oceanic fabric and the slab strike approaches 30°. In the detailed data set available for the Aleutian Trench, faults controlled by the oceanic fabric are dominant along most of the central trench, but a new set of slab-parallel faults begin to develop at the eastern trench when the degree of obliquity between oceanic fabric and slab strike reaches about 25° (Figure 7). This new fault set then increases in importance (in an irregular manner) as the obliquity increases to 30°, by which point it has become the dominant trend. Unfortunately, 30° is the greatest degree of obliquity seen at the Aleutian

Trench, so the continued development of the fault zone with increasing obliquity between slab strike and oceanic fabric cannot be resolved. However, at the Java Trench, where the two trends are oblique by exactly 30°, no re-activation of the oceanic fabric is seen. This suggests that 30° of divergence between fault trend and stress directions is the maximum which can be accommodated, and that beyond that, a new fault set has to develop.

A characteristic of the areas examined in this study is that fault zones controlled by re-activation of the oceanic spreading fabric show a distinctly narrower range of fault trend ($\sim 20°$, e.g. Figure 10) than fault zones where a new set of faults, perpendicular to the principal stress direction, is formed ($\sim 35°$, e.g. Figure 11). This can be clearly seen by comparing fault distributions along the western and central segments of the Aleutian Trench (Figure 9, top and middle) or by comparing data from the Peru Trench with that from the Java and Tonga Trenches (Figure 10 with Figures 11, 12). There is no direct evidence as to the cause of this phenomenon, although one might reasonably assume that it relates to the different response to extension of lithosphere at mid-ocean ridges, when the oceanic spreading fabric is created, to that of lithosphere adjacent to trenches where old lithosphere is being subducted. Clearly the thickness and strength of the lithosphere in the two environments is very different, and it might be speculated that the weaker lithosphere at mid-ocean ridges fractures more precisely in response to the extensional stress than does the older, stronger lithosphere away from the ridges. However, further study of the topic is required before a full explanation can be given.

Acknowledgements

I would like to thank all the scientists who assisted with the collection of the data used in this study, particularly those from the U.S. Geological Survey and the U.K. Institute of Oceanographic Sciences who participated in the Aleutian Arc studies. Funding for part of the Tonga Trench data collection was provided by the Defence Scientific Establishment, New Zealand Ministry of Defence. Reviews of the manuscript by L. M. Parson, R. B. Whitmarsh and three journal reviewers are gratefully acknowledged.

References

AAPG, 1982, Plate Tectonic Maps of the Circum-Pacific Region. Amer. Assoc. Petroleum Geol., Tulsa, Oklahoma.

AAPG, 1984, Geodynamic Maps of the Circum-Pacific Region. Amer. Assoc. Petroleum Geol., Tulsa, Oklahoma.

Aubouin, J., Stephen, J.-F., Renard, V., Roump, J. and Lonsdale, P., 1982, a Seabeam Survey of the Leg 67 Area (Middle America Trench off Guatemala) in Aubouin, J., von Huene, R. *et al.* (eds.), Initial Reports Deep Sea Drilling Project, 67. U.S. Government Printing Office, Washington, D.C., pp. 733–738.

Aubouin J., Bourgois, J., and Azema, J., 1984, A New Type of Active Margin: The Convergent-Extensional Margin, as Exemplified by the Middle America Trench Off Guatemala, *Earth Planet. Sci. Lett.* **67**, 211–218.

Barazangi, M. and Isacks, B. L., 1976, Spatial Distribution of Earthquakes and Subduction of the Nazca Plate Beneath South America, *Geology* **4**, 686–692.

Cadet, J. -P., Kobayashi, K., Aubouin, J., Boulegue, J., Deplus, C., Dubois, J., von Huene, R., Jolivet, L., Kanazawa, T., Kasahara, J., Koizumi, K., Lallemand, S., Nakamura, Y., Pautot, G., Suyehiro, K., Tani, S., Hidekazu, T., and Yamazaki, T., 1987, The Japan Trench and its Juncture with the Kuril Trench: Cruise Results of the Kaiko Project, Leg 3. *Earth Planet. Sci. Letters* **83**, 267–284.

Heirtzler, J. R., Cameron, P., Cook, P. J., Powell, T., Roeser, M. A., Sukardi, S., and Veevers, J. J., 1978, The Argo Abyssal Plain, *Earth Planet. Sci. Letters* **41**, 21–31.

Hey, R. N., 1977, A new class of 'pseudofault' and their bearing on plate tectonics: a propagating rift model, *Earth Planet. Sci. Letters* **37**, 321–325.

Hilde, T. W. C., 1983, Sediment Subduction versus Accretion Around the Pacific, *Tectonophysics* **99**, 381–397.

Jones, G. M., Hilde, T. W. C., Sharman, G. F., and Agnew, D. C., 1978, Fault Patterns in Outer Trench Walls, *J. Phys. Earth* **26**, suppl. S85–S101.

Kaiko 1 Research Group, 1986, Topography and Structure of Trenches Around Japan—Data Atlas of Franco-Japanese Kaiko project, phase 1, Ocean Res. Institute, Tokyo and IFREMER, Paris.

Klitgord, K. D. and Mammerickx, J., 1982, Northern East Pacific Rise: Magnetic Anomaly and Bathymetric Framework, *J. Geophys. Res.* **87**, 6725–6750.

Kobayashi, K., Cadet, J. -P., Aubouin, J., Boulegue, J., Dubois, J., von Huene, R., Jolivet, L., Kanazawa, T., Kasahara, J., Koizumi, K., Lallemand, S., Nakamura, Y., Pautot, G., Suyehiro, K., Tani, S., Tokuyama, H., and Yamazaki, T. 1987. Normal faulting of the Daiichi-Kashima Seamount in the Japan Trench Revealed by the Kaiko 1 Cruise, Leg 3. *Earth Planet. Sci. Letters* **83**, 257–266.

Le Pichon, X. and Huchon, P., 1987, Central Japan Triple Junction Revisited, *Tectonics* **6**, 35–46.

Lonsdale, P., 1986, A Multibeam Reconnaissance of the Tonga Trench Axis and its Intersection with the Louisville Guyot Chain, *Marine Geophys. Res.* **8**, 295–327.

Lonsdale, P., 1988, Palaeogene History of the Kula Plate: Offshore Evidence and Onshore Implications, *Geol. Soc. America Bull.* **100**, 733–754.

Ludwig, W. J., Ewing, J. I., Ewing, M., Murauchi, S., Den, N., Asano, S., Hotta, H., Hayakawa, M., Asanuma, T., Ichikawa, K., and Noguchi, I., 1966, Sediments and Structure of the Japan Trench, *J. Geophys. Res.* **71**, 2121–2137.

Masson, D. G., Parson, L. M., Milsom, J., Nichols, G., Sikumbang, N., Dwiyanto, B., and Kallagher, H., 1990, Subduction of Seamounts at the Java Trench—a View with Long-Range Sidescan Sonar, *Tectonophysics* **185**, 51–65.

McCaffrey, R., Molnar, P., and Roecker, S. W., 1985, Microearthquake Seismicity and Fault Plane Solutions Related to Arc-Continent Collision in the Eastern Sunda Arc, Indonesia, *J. Geophys. Res.* **90**, 4511–4528.

Moore, G. F. and Shipley, T. H., 1988, Mechanisms of Sediment Accretion at the Middle America Trench off Mexico, *J. Geophys. Res.* **93**, 8911–8928.

Nixon, G. T., 1982, The Relationship Between Quaternary Volcanism in Central America and the Seismicity and Structure of Subducted Ocean Lithosphere, *Geol. Soc. America Bull.* **93,** 514–523.

Parson, L. M., 1989, *Geophysical and Geological Investigations of the Lau Backarc Basin, SW Pacific*, IOS Cruise Report 206, 28 pp.

Pilger, R. H., 1983, Kinematics of the South American Subduction zone from Global Plate Reconstructions, in S. J. Ramon Cabre (ed.), *Geodynamics of the Eastern Pacific Region, Caribbean and Scotia Arcs*, Geodynamics Series 9, American Geophys. Union, Washington, D.C. and Geol. Soc. America, Boulder, Colorado, pp. 113–126.

Renard, V., Nakamura, K., Angelier, J., Azema, J., Bourgois, J., Deplus, C., Fujioka, K., Hamano, Y., Huchon, P., Kinoshita, H., Labaume, P., Ogawa, Y., Seno, T., Takeuchi, A., Tanahashi, M., Uchiyama, A., and Vigneresse, J. -L. 1987, Trench Triple Junction off Central Japan—Preliminary Results of French-Japanese 1984 Kaiko Cruise, Leg 2. *Earth Planet. Sci. Letters* **83**, 243–256.

Scholl, D. W., Vallier, T. L., and Stevenson, A. J., 1982, Sedimentation and Deformation in the Amlia Fracture Zone Sector of the Aleutian Trench, *Marine Geology* **48**, 105–134.

Shipley, T. H. and Moore, G. F., 1985, Sediment accretion and subduction in the Middle America Trench, in Nasu, N., Kobayashi, S., Uyeda, S., Kushiro, I., and Kagami, H. (eds.), *Formation of Active Ocean Margins*, Terra Scientific Publishing, Tokyo, pp. 221–225.

Shipley, T. H., McMillen, K. J., Watkins, J. S., Moore, J. C., Sandoval-Ochoa, J. H., and Worzel, J. L., 1980, Continental Margin and Lower Slope Structures of the Middle America Trench near Acapulco (Mexico), *Marine Geol.* **35**, 65–82.

Stone, D. B., 1988, Bering Sea-Aleutian Arc, Alaska, in A. E. M. Nairn, F. G. Stehli, and S. Uyeda (eds.), *The Ocean Basins and Margins, 7B, The Pacific Ocean*, Plenum Press, New York, pp. 1–84.

Vasicek, J. M., Frey, H. V., and Thomas, H. H., 1988, Satellite Magnetic Anomalies and the Middle America Trench, *Tectonophysics* **154**, 19–24.

Warsi, W. E. K., Hilde, T. W. C., and Searle, R. C., 1983, Convergence Structures of the Peru Trench Between 10° S and 14° S, *Tectonophysics* **99**, 313–329.